0273-2289/97/63-65—0743$11.75

Observations of Metabolite Formation and Variable Yield in Thiodiglycol Biodegradation Process

Impact on Reactor Design

TSU-SHUN LEE,[1,2] WILLIAM A. WEIGAND,[2] AND WILLIAM E. BENTLEY*,[1,2]

[1]*Center for Agricultural Biotechnology, University of Maryland Biotechnology Institute; and* [2]*Department of Chemical Engineering, University of Maryland, College Park, MD 20742*

ABSTRACT

The complete microbial degradation of thiodiglycol (TDG), the primary hydrolysis product of sulfur mustard, by *Alcaligenes xylosoxydans* ssp. *xylosoxydans* (SH91) was accomplished in laboratory-scale stirred-tank reactors. An Andrews substrate inhibition model was used to describe the cell growth. The yield factor was not constant, but a relationship with initial substrate concentration has been developed. Using a substrate-inhibition and variable-yield kinetic model, we can describe the cell growth and substrate consumption in batch and repeated batch fermentations. Several reactor-operating modes successfully degrade TDG concentration to below 0.5 g/L. According to the experimental results, the two-stage repeated batch operation has the best degradation efficiency, and it also can degrade 500 m*M* TDG (≈60 g/L) to 5 m*M* (≈0.7 g/L) in <5 d. A hypothesis for explaining variable-yield and byproduct formation based on the capacity and utilization of metabolic loads is presented.

Index Entries: Biodegradation; thiodiglycol; sulfur mustard; metabolic model.

*Author to whom all correspondence and reprint requests should be addressed.

INTRODUCTION

Biodegradation is the method that uses biological means for waste treatment. This technology has become increasingly important, not only for industrial hazardous chemical disposal, but also for chemical warfare agent disposal. This method has several advantages. First, it is the most economic method for toxic waste mineralization. For example, biodegradation processes cost \$40–70/t of waste, whereas incineration processes are almost 10 times higher. Second, it is environmental friendly, because the pollutant is naturally degraded to innocuous products, such as CO_2, H_2O, and microorganisms. Finally, biodegradation is a natural process, which makes it easier for the public to accept. Accordingly, our lab has evaluated the biodegradation of thiodiglycol (TDG), the main hydrolysis product of sulfur mustard.

Sulfur mustard, a chemical warfare agent, can be hydrolyzed in water *(1)*, forming hydrochloric acid and TDG. Yang and others have investigated the aqueous hydrolysis reaction kinetics *(2)*. Compared to sulfur mustard, TDG is relatively nontoxic; the LD_{50} (dose at which 50% lethality is effected) of TDG varies from 3000–6610 mg/kg, depending on the species *(3)*. This level of toxicity is similar to isopropanol. TDG has many industrial uses, for example, it is used in elastomers, lubricants, stabilizers, antioxidants, inks, dyes, and so forth. Although TDG is relatively nontoxic and has many industrial uses, it can also be used to manufacture sulfur mustard. TDG is listed in the chemical weapon convention treaty *(4)* and must be degraded in a sulfur mustard mineralization process.

In this article, *Alcaligenes xylosoxydans* ssp. *xylosoxydans* (SH91), a Gram-negative bacterium that consumes TDG as the sole carbon source, was employed. In previous papers, an Andrews-type inhibition model with constant yield was used to describe SH91 growth on TDG-based media *(5,6)*. In the present work, simulations based on the previous model were compared to experiments with high initial TDG concentration (≥80 m*M*, 10 g/L). As the initial TDG concentration increased, so did the deviation between model and experiment. By HPLC analysis, the amounts of metabolic byproduct increased with initial TDG concentration. The specific growth rate and cell mass yield were affected by these metabolites, so an improved Andrews inhibition model incorporating a variable cell mass yield was developed and is presented here. Also, several different batch-type operating strategies were used to degrade TDG. An evaluation of these operating modes is included. Finally, a new model is proposed based on the cell's metabolic capacity for degrading TDG and its metabolites. The model qualitatively describes the variable-yield phenomena noted in our experiments.

POSSIBLE DEGRADATION PATHWAY

TDG was injected into rats, and was metabolized into TDG sulfoxide (TDGS), TDG sulfone, and so forth *(7)*. The initial step of TDG degradation by SH91 was determined by Zulty et al. *(8)*, TDG is converted to *S*-(2-

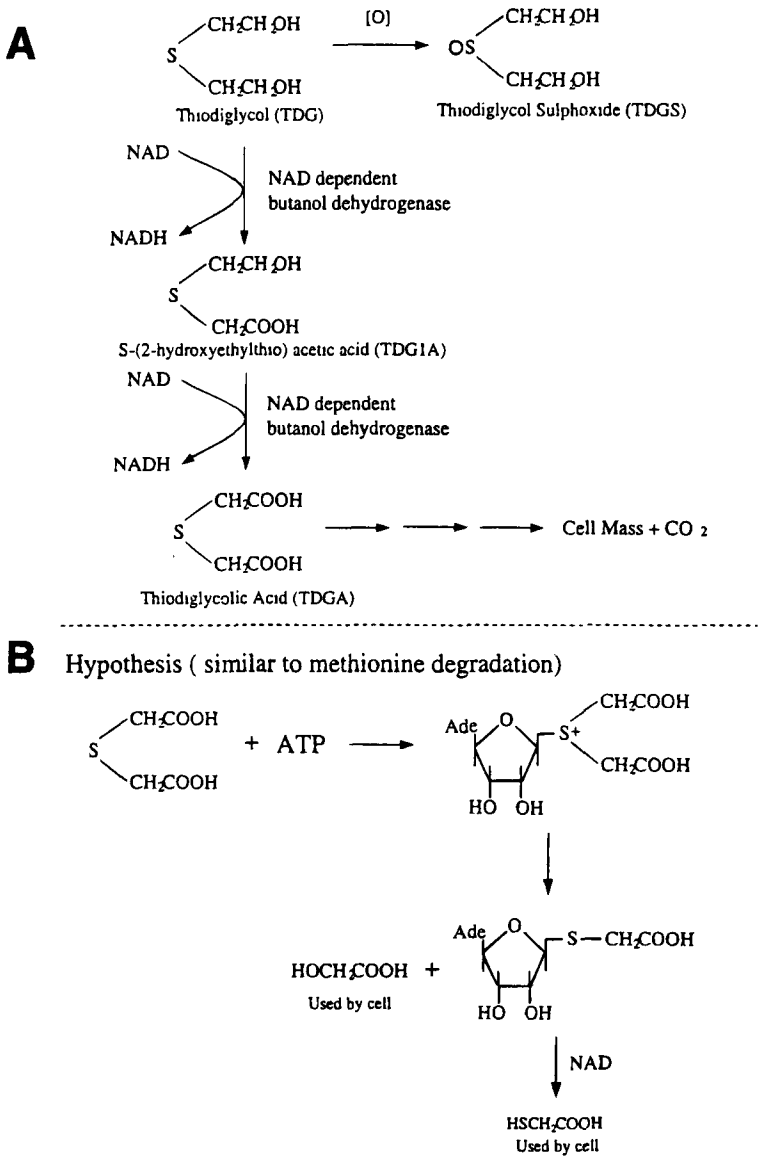

Fig. 1. The metabolic pathway for SH91 to degrade TDG. **(A)** SH91 use NAD-dependent butanol dehydrogenase to convert TDG to TDG1A, and TDG1A to TDGA. The other degradation pathway is TDG oxidized by oxygen to produce TDGS. **(B)** The possible TDGA degradation pathway (hypothesis based on methionine degradation).

hydroxyethylthio) acetic acid (TDG1A). The enzyme used to catalyze this reaction is NAD-dependent butanol dehydrogenase. This enzyme is used again to convert *S*-(2-hydroxyethylthio) acetic acid to TDG acid (TDGA). Two NADH are produced in these steps. Additionally, we found that TDG is oxidized by molecular oxygen yielding TDGS, which is detected by HPLC. The proposed metabolic pathway is summarized in Fig. 1A. Based

on methionine degradation pathways elucidated in *Escherichia coli* bacteria, we suggest an analogous metabolic pathway is used for TDGA in SH91, as shown in Fig. 1B. This is consistent with our metabolic byproduct analyses.

MATERIALS AND METHODS

Microorganism, Media, and Culture Conditions

A. xylosoxydans ssp. *xylosoxydans* (SH91), a Gram-negative bacterium, uses TDG as the sole carbon source for growth. Stock cultures were maintained on TDG medium, which has the following composition (per liter): TDG, 3.66 g (30 m*M*); ammonium sulfate, 2 g (15.1 m*M*); potassium phosphate dibasic 2 g (11.5 m*M*); and modified Wolin salts solution 10 mL (WS42). The composition of WS42 was (per liter): nitrilotriacetic acid, 3 g (15.7 m*M*; add NaOH until dissolved); $MgSO_4 \cdot 7H_2O$, 6 g (24.3 m*M*); NaCl, 1 g (17.1 m*M*); $MnSO_4 \cdot H_2O$, 1 g (5.9 m*M*); $FeSO_4 \cdot 7H_2O$, 0.5 g (1.8 m*M*); $CaCl_2 \cdot 2H_2O$, 0.1 g (0.68 m*M*); $CoCl_2 \cdot 6H_2O$, 0.1 g (0.42 m*M*); $ZnSO_4 \cdot 7H_2O$, 0.1 g (0.35 m*M*); H_3BO_3, 0.02 g (0.32 m*M*) $Na_2MoO_4 \cdot 2H_2O$, 0.01 g (0.04 m*M*); $CuSO_4$, 0.01 g (0.06 m*M*). Finally, NaOH was used to adjust the pH of TDG medium to 9.2. The best growth conditions were 30°C and pH-8.0. Cells were transfered to fresh TDG medium every 4 d in order to sustain exponential growth. Inoculum was prepared by adding 4 mL SH91 freezer stock to 250-mL shake flasks with 100 mL TDG medium. This was incubated for 3 d in a reciprocating shaker at 30°C and 150 rpm. Thereafter it was added to the fermenters (New Brunswick Scientific, Hatfield, UK).

Analytical Methods

Cell concentration was determined by optical density (OD_{590}, Milton Roy, FL, Spec21). The absorbance of the background media was used to correct the absorbance readings. Dry cell weights were directly proportional to optical density up to 0.4 OD_{590} (conversion factor = 0.8 g/OD_{590} · L). Samples above 0.4 OD_{590} were diluted into the linear range with deionized water.

TDG, TDG1A, TDGA, TDGS were determined by HPLC (Waters Model 590) at 214 nm (Waters, UV detector) with a Pham-Pak column *(9)*. TDG and TDGA standards were purchased from Sigma Chemical Co. St. Louis, MO). TDGS standard was prepared by addition of 30% H_2O_2 to TDG *(7)*. The HPLC running conditions were as follows: column temperature, 65°C; mobile phase, 3 m*M* phosphoric acid (flow rate: 1 mL/min.). The linear range for TDG, TDGA, and TDGS was 0.3–10 m*M*, 0.5–20 m*M*, and 0.5–15 m*M*, respectively. All samples taken from the fermenter were filtered (0.2 μm) before injection. *See* Table 1 for typical results.

Reactor Operation

Batch fermentations were run in a 700-mL BioFlo I fermenter with a 500-mL working volume and 2-L BioFlo I fermenter with a 1.5-L working

Table 1
The Accumulated Metabolite Concentrations
in Four Different Batch Final Broths

	30 mM	60 mM	120 mM	170 mM
TDG (mM)	0	0	0	0
TDG1A (mM)	0	0	0.5	17.18
TDGA (mM)	0	3.02	17.4	60.34
TDGS (mM)	2.4	3.89	6.91	6.84
Total (mM)	2.4	6.91	24.86	84.36

volume (New Brunswick Scientific, Inc.). The agitation rate was 400 rpm, and the inlet air was sterilized by a 0.2-μm filter. The inlet air was humidified by passing through a water bath to avoid evaporation. Temperature and pH were controlled at 30°C and 80°, respectively. There are four different fermentation operating policies as shown in Fig. 2. They are batch, repeated batch, two-stage batch, and fed batch with linear feed. For repeated batch, two different TDG feed concentrations were employed (60 and 270 m*M*). For the 60-m*M* case, fresh TDG medium was fed into the bioreactor after an initial batch phase (increase from 250–500 mL), and the reactor was run batchwise until all TDG was consumed (≈48 h). Then, 250 mL medium was withdrawn, 250 mL fresh 60 m*M* TDG medium was added, and a new cycle was begun. This cyclic process was run until 10 L (60 m*M*) of TDG medium was processed. For the 270–m*M* case, we followed almost the same procedure. Initially, 1 L of fresh TDG medium was added into the reactor with 0.5 L broth (1.5 L), and a new cycle was begun (cycle time: 60 h). Then, 1 L of fresh TDG medium was withdrawn and replaced with fresh media at every cycle. The two-stage batch was divided into two batch processes as shown in Fig. 2. First, 250 mL fresh 500 m*M* TDG medium was added into a reactor (from 500 to 750 mL), and the reactor was run batchwise for 2 d. Then, 500 mL fresh 500 m*M* TDG medium were added, and again the reactor was run batchwise until TDG was consumed to the desired level (3 d). The final batch-type operating mode was fed batch with linear feed. It was divided into three periods. They were feeding, reacting, and withdrawing. In 24 h the reactor volume was increased steadily from 500 to 1500 mL (flow rate: 41.67 mL/h), at which time the reactor was run batchwise for the remaining time (60 h). The withdrawal period was fast (≈10 min), so it was neglected in modeling calculations (Fig. 2). Three complete cycles were run.

MATHEMATICAL MODEL

The model used to describe SH91 growth in TDG medium is an Andrews-type substrate-inhibition model *(10)*:

$$\mu(s) = [\mu_{max}/(1 + (K_s/s) + (s/K_i))] \quad (1)$$

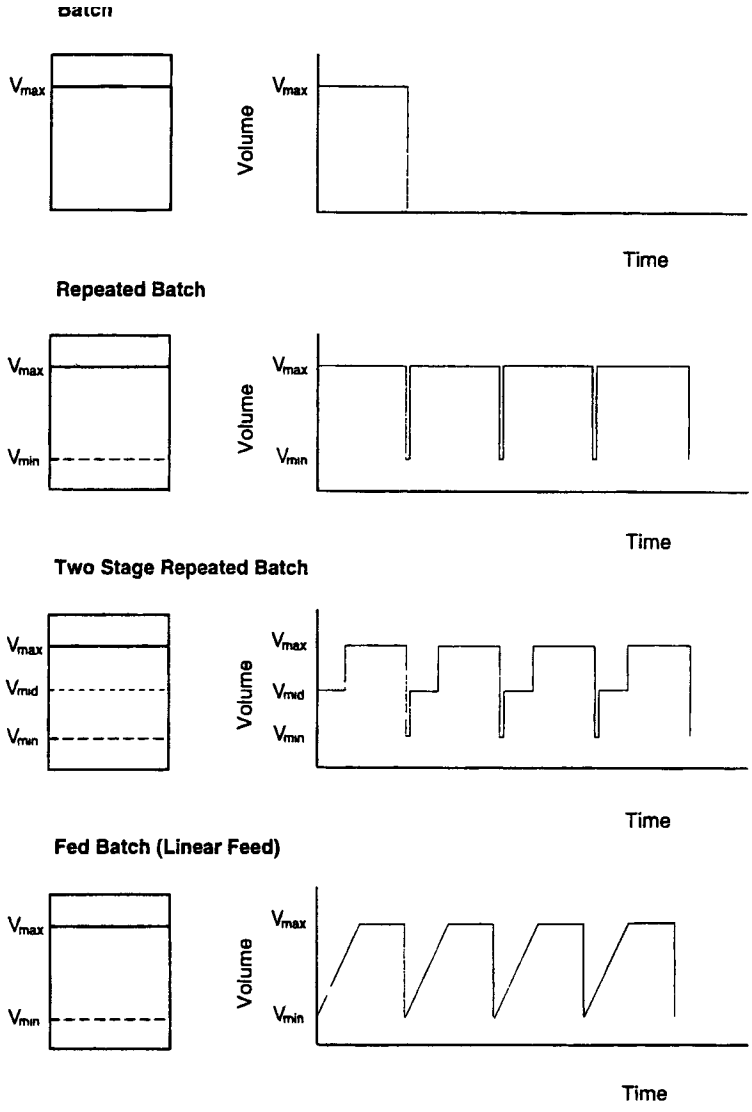

Fig. 2. Four different kinds of batch fermentation. They are batch, repeated batch, two-stage repeated batch, and fed batch.

where s is the growth-limiting substrate (TDG) concentration (g/L), μ_{max} is the maximum specific growth rate (1/h), K_s is the substrate saturation constant (g/L), and K_i is the substrate inhibition constant (g/L). The cell growth is described by an autocatalytic reaction including cell death:

$$(dx/dt) = \mu(s)x - k_d x \tag{2}$$

where k_d is the death rate constant (1/h) as measured previously (*5*). During cell growth, the substrate is simultaneously consumed:

$$(ds/dt) = (-1/Y_{x/s})\mu(s)x \tag{3}$$

Table 2
Model Parameters

Parameter	Value
Maximum Growth Rate (μ_{max})	0.171(1/hr)
Substrate Constant (K_s)	2.77 g/L (49.45 mM)
Inhibition Constant (K_i)	9.47 g/L (81.68 mM)
Death Rate Constant (k_d)	7.8×10^{-3}(1/hr)
Yield Factor ($Y_{x/s}$)	Variable
Max. Yield Factor ($Y^M_{x/s}$)	0.345 (g/g)

where ds/dt is the substrate accumulation rate (g/L · h), and $Y_{x/s}$ is the apparent yield factor. In the present work, the yield coefficient is a function of initial TDG concentration:

$$Y_{x/s} = 0.345\ e^{-0.5s} \tag{4}$$

These four equations were used to simulate SH91 growth in TDG. All the parameters are listed in Table 2.

SIMULATION AND EXPERIMENTAL RESULTS

A series of batch fermentations with different initial TDG concentrations was run to determine cell mass yield and specific growth rate. The calculated yield coefficient (obtained from the slope of OD vs S plots) was not constant. Instead, it decreased with increased initial TDG concentration. Interestingly, the yield was constant over the time-course of a fermentation, but varied depending on the initial concentration. For simplicity, an exponential decay function was used to fit the experimental data (Fig. 3). The specific growth rates diverge at initial TDG concentration above 10 g/L, as shown in Fig. 4. In our previous studies, the specific growth rate observed at high TDG was from shake flasks without pH control. The specific growth rate determined here was measured from batch reactors with pH control. Additionally, the bioreactor data were obtained in a single extended repeated batch experiment, where the inoculum for the next experiment was the material left after draw-down of 90% of the reactor volume from the previous experiment. As will be addressed later, this method retains 10% of the metabolic byproducts produced during the batch. This, in addition to the pH control (which in isolated batch cultures yields more metabolites; not shown), provides a basis for why the growth rate is different at high initial TDG (more metabolites produced per TDG). The three calculated kinetic parameters are μ_{max}, K_S, and K_i, and their values are 0.171/h$^-$, 2.77 g/L (22.68 mM/L), and 9.47 g/L (77.51 mM/L), respectively. The parameters from our previous studies were 0.277 h^{-1} (μ_{max}), 6.04 g/L (K_S), and 9.98 g/L (K_i). The new specific growth rate is

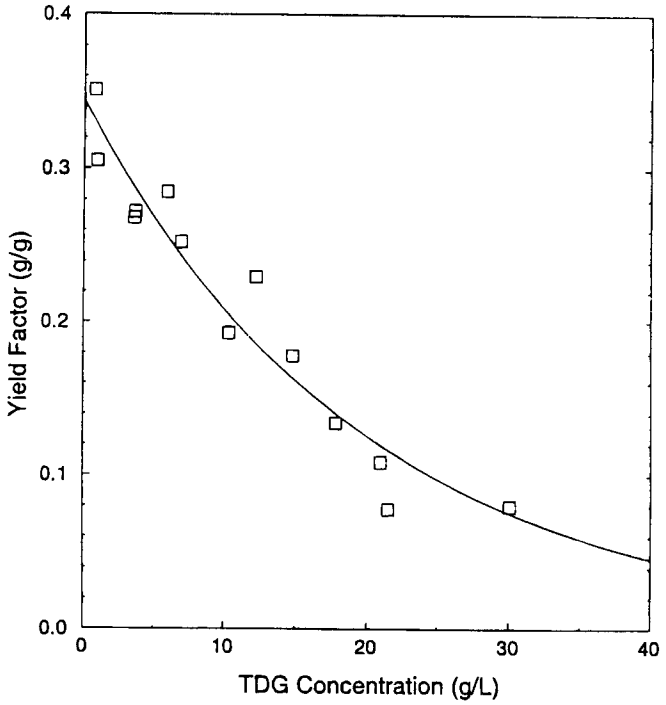

Fig. 3. The yield factor is a function of TDG concentration: $y_{x/s} = 0.345 \times \exp. - 0.05s$ (s = *TDG* conc. g/L).

lower than the previous rate when TDG concentrations are higher than 5 g/L (40 m*M*). Again this is likely owing to the production of the metabolic byproducts, which affects the TDG consumption rate and, thus, cellular specific growth rate.

The simulation and experimental results for batch reactors are shown in Fig. 5. Four different initial TDG concentration results are shown. Also, the previous and new model simulation results are depicted. As expected, both the new and old models described low TDG (≤60 m*M*, 7.3 g/L) batch experiments quite well (Fig. 5A,B). The previous model failed to describe high TDG concentration batch experiments, whereas the new model was in good agreement with the experimental data up to 20 g/L (170 m*M*), as shown in Fig. 5C,D. In Table 1, the metabolite accumulation was more problematic as TDG concentration was increased (refer to Fig. 1A). We further employed the model to simulate 60- and 270-m*M* repeated batch fermentations (Fig. 6). The new model parameters and variable-yield calculations described the 60-m*M* repeated batch process as well as or better than the previous model *(5)*. However, the new model still deviated from experimental results for a 270-m*M* repeated batch process. Note, however, that for the 270-m*M* repeated batch experiment, we found significantly more TDG1A and TDGA in the broth at the end of each cycle than for the previous batches

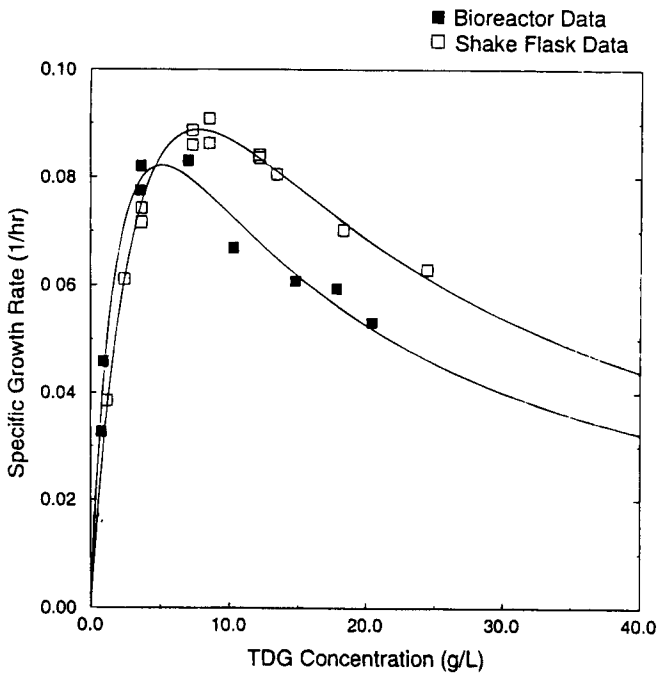

Fig. 4. Andrews inhibition model fit to results of shake flask and bioreactor experimental data: shake-flask model result (K_S = 6.04 g/L [49.45 m*M*], K_i = 9.98 g/L [81.68 m*M*], μ_{max} = 0.227 [h^{-1}]), bioreactor model results (K_S = 2.77 g/L [22.67 m*M*], K_i = 9.47 g/L [77.51 m*M*], μ_{max} = 0.171 [h^{-1}]).

(30–170 m*M*; *see* Tables 1–4). Thus, we hypothesized that several metabolic interactions were at play in this system:

1. High initial TDG resulted in more metabolic byproduct production;
2. High levels of metabolic byproducts in the media were detrimental to cell growth; and
3. Decreased cell growth also meant decreased specific TDG uptake.

Several additional repeated batch operating policies were developed and run to test these interactions. Two-stage batch experimental results are shown in Fig. 7A. Overall, this method degraded TDG from 500 (60 g/L) to 1.1 m*M* (0.13 g/L) in 120 h. For the first stage, 500 m*M* TDG was added, increasing the volume from 500 to 750 mL. It took 48 h to degrade TDG from 170 (20.7 g/L) to 9.7 m*M* (1.2 g/L), when cell mass increased from 2.4 to 3.5 g/L. From HPLC chromatograms, significant levels of metabolite had accumulated (not shown). For the second stage, 500 m*M* TDG was added to the reactor, increasing the volume from 750 to 1500 mL (maximum value). It took 72 additional hours to degrade TDG from 250 (30.5 g/L) to 1.1 m*M* (0.13 g/L). The cell mass increased from 1.89 to 4.42 g/L. From HPLC chromatograms, a large amount of both TDG1A and TDGA had accumulated in the reactor (*see* Table 4).

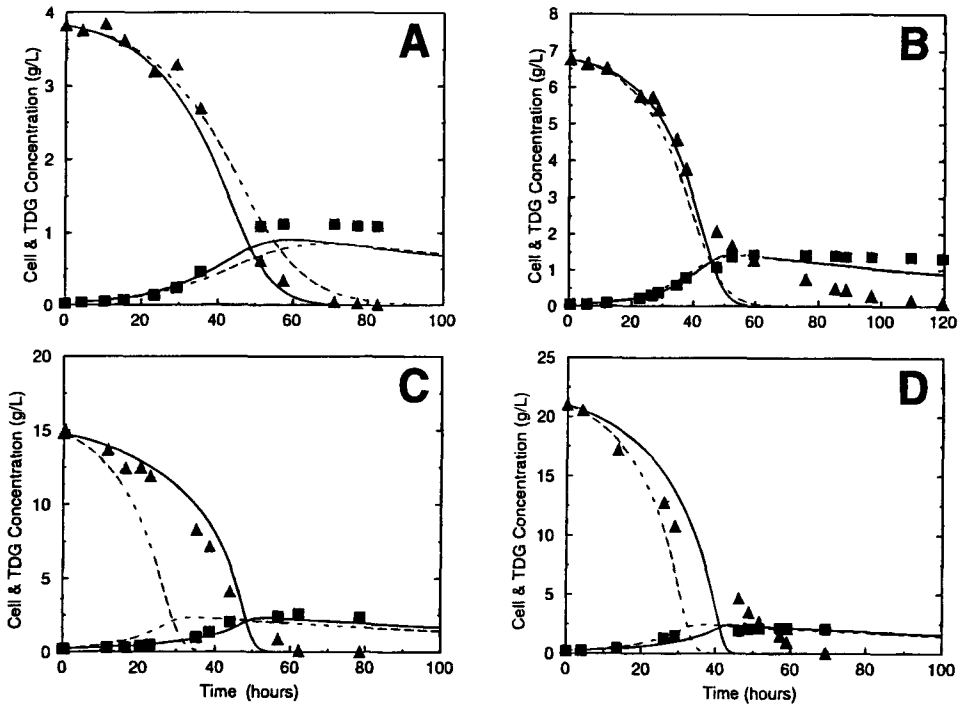

Fig. 5. Four different initial TDG concentration batch experimental and simulation results (dash line: old model; solid line: new model): **(A)** 30-m*M* batch, **(B)** 60-m*M* batch, **(C)** 120-m*M* batch, and **(D)** 170-m*M* batch.

Table 3
Degradation Index for Three Batch-Type Bioreactors
(First-Calculation Method)

	270mM RB	500mM TSRB	300mM RFB
Influent TDG (mM)	270	512	290
effluent TDG (mM)	0	6.55	4.26
Withdraw volume	1000 ml	1000 ml	1000 ml
Max working volume	1500 ml	1500 ml	1500 ml
Spending time	60 hrs	120hrs	84 hrs
DI (mM/hr)	3.0	2.8	2.3

The results for a linear-feed repeated fed-batch reactor are shown in Fig. 7B. During the 24-h feeding period (41.67 mL/h), TDG concentration increased from 3 (0.36 g/L) to near 130 m*M* (15.88 g/L), and cell mass decreased slightly owing to dilution. For the remaining batch periods, the TDG decreased from 130 to 4.4 m*M*, and cell mass gradually increased from 1.9 to 2.5 g/L. As mentioned earlier, metabolites accumulated in the broth (*see* Table 4).

The overall degradation index (DI) was calculated for repeated batch, two-stage batch, and repeated fed-batch reactors. Two different calcula-

Table 4
Degradation Index for Three Batch-Type Bioreactors
(Second-Calculation Method)

	270mM RB	500mM TSRB	300mM RFB
Influent TDG (mM)	270	512	290
effluent TDG (mM)	0	6.55	4.26
Metabolites (mM)	118.27	162.78	58.95
Withdraw volume	1000 ml	1000 ml	1000 ml
Max working volume	1500 ml	1500 ml	1500 ml
Spending time	60 hrs	120hrs	84 hrs
DI (mM/hr)	1.7	1.9	1.8

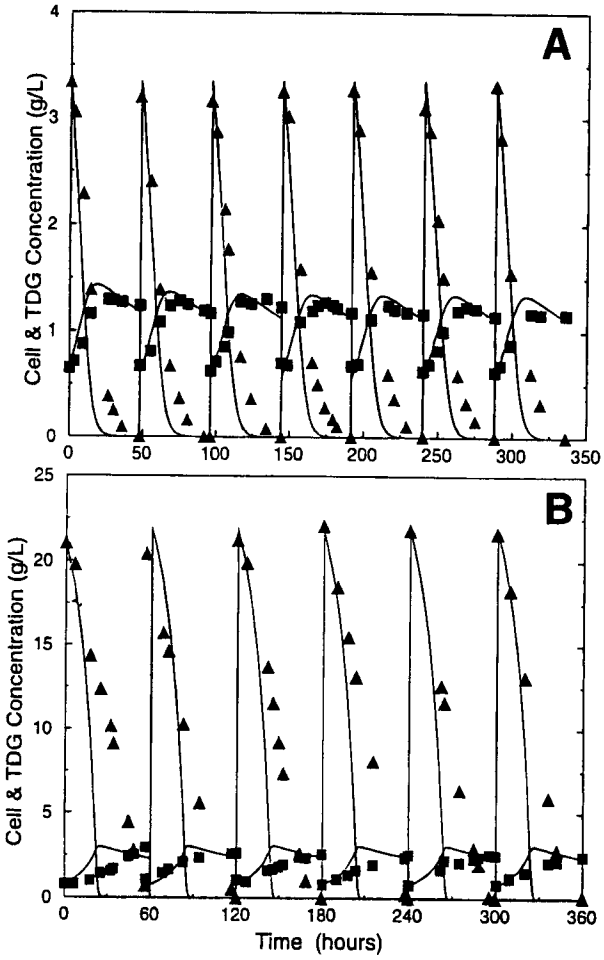

Fig. 6. Two different repeated batch experimental and simulation results: **(A)** 60-m*M* repeated batch and **(B)** 270-m*M* repeated batch.

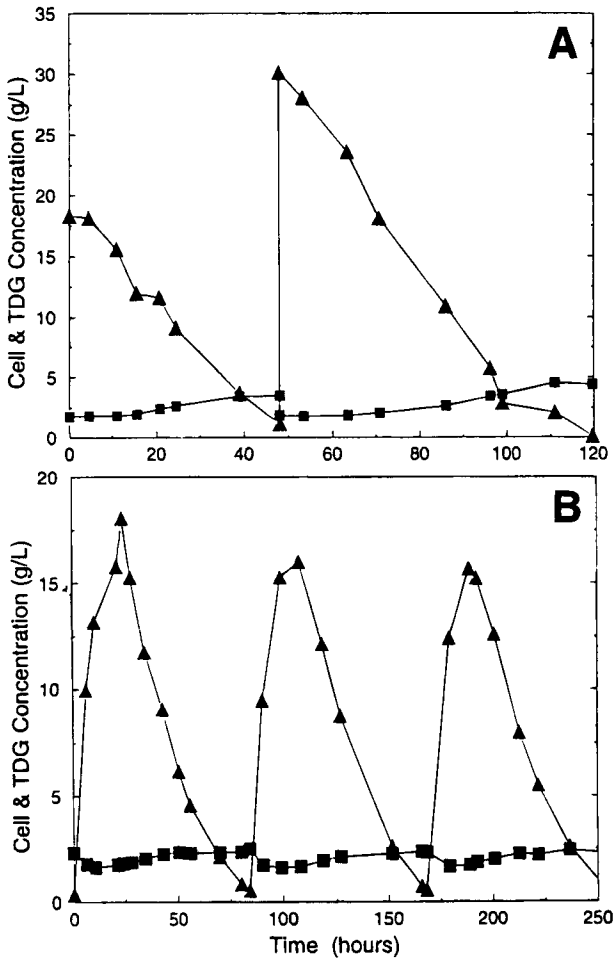

Fig. 7. **(A)** Two-stage batch experimental result and **(B)** repeated fed-batch experimental results.

tion methods are presented here. The first method focuses on TDG degradation, and does not account for the metabolites produced by SH91 during growth. The calculation is as follows:

$$DI = \left[\left(TDG_{inf} - TDG_{eff}\right) \times V_{wd} / V_{max} \times T_f\right] \quad (5)$$

where DI is degradation index, TDG_{inf} and TDG_{eff} are influent and effluent TDG concentration, V_{wd} is the withdrawn volume, V_{max} is the maximum working volume, and T_f is total operating time (*see* 9).

The other method focuses on the amount of TDG completely degraded by SH91. The calculation is as follows:

$$DI = \left[\left(TDG_{inf} - TDG_{eff} - M_{eff}\right) \times V_{wd} / V_{max} \times T_f\right] \quad (6)$$

where M_{eff} is the concentration of accumulated metabolites, including TDG1A, TDGA, and TDGS. The results for these two methods are listed in Table 3 (based on Eq. 5) and Table 4 (based on Eq 6).

DISCUSSION

The simulation results for an Andrews inhibition model with new parameters agree quite well for different batch reactor schemes. The simulation results are significantly improved for high concentrations of TDG (≤120 m*M*, 14.7 g/L) as shown in Fig. 5C,D. Note at least 600 m*M* TDG are likely to remain after mustard hydrolysis. Some deviation was found between experimental and simulation results in the 270-m*M* repeated batch, especially for the TDG consumption rate. The predicted rate was more rapid than the actual consumption rate. For the 270-m*M* repeated batch, the initial thiodiglycol concentration was near 170–180 m*M* or was almost the same as the 170-m*M* batch fermentation. Accordingly, they should have the same kinetic result. The reason for the model failure when describing the 270-m*M* repeated batch is the influence of metabolite accumulation. From our HPLC chromatograms, we found the TDG1A concentration in 270-m*M* repeated batch was 2.5× higher than the 170-m*M* batch reactor. TDG and TDG1A are substrates for the same enzyme, so TDG1A competes with TDG for the NAD-dependent butanol dehydrogenase, as shown in Fig. 1. Thus, the amount of TDG1A directly affects the TDG degradation rate; the more TDG1A is accumulated in the bioreactor, the more the TDG consumption rate is reduced. This phenomenon was also observed in the 500-m*M* two-phase batch and repeated fed-batch cases.

There are two different goals or paradigms for TDG degradation. The first focuses on TDG alone, and the metabolites produced by SH91 are neglected. For this paradigm, we found the 270 m*M* repeated batch reactor provided the best degradation efficiency, and the 300 m*M* repeated fed-batch reactor was the worst. The second paradigm focuses on the amount of TDG completely degraded (i.e., to biomass, CO_2, H_2O, inorganics). In this case, we found the two-stage batch was best, although the 300-m*M* repeated fed batch was a close second. For the 270-mM repeated batch reactor, much TDC was converted to TDG1A and TDGA, which slowed the overall process down. For the 300-m*M* fed batch, TDG was continuously introduced, and the TDG concentration increased gradually. Correspondingly, the cells had more time to completely degrade TDG. They were not exposed to as high a TDG concentration in as short a time, so the problem of TDG1A and TDGA accumulation was less serious than with the 270-mM repeated batch. The two-phase batch is midway between a fed-batch and batch scheme, since it divides a batch into two separated batches. It avoids sudden exposure to very high TDG concentration, which has two beneficial effects: first, it reduces the substrate inhibition for cell growth, and second, it produces less metabolite (TDG1A) that competes for the same enzyme as

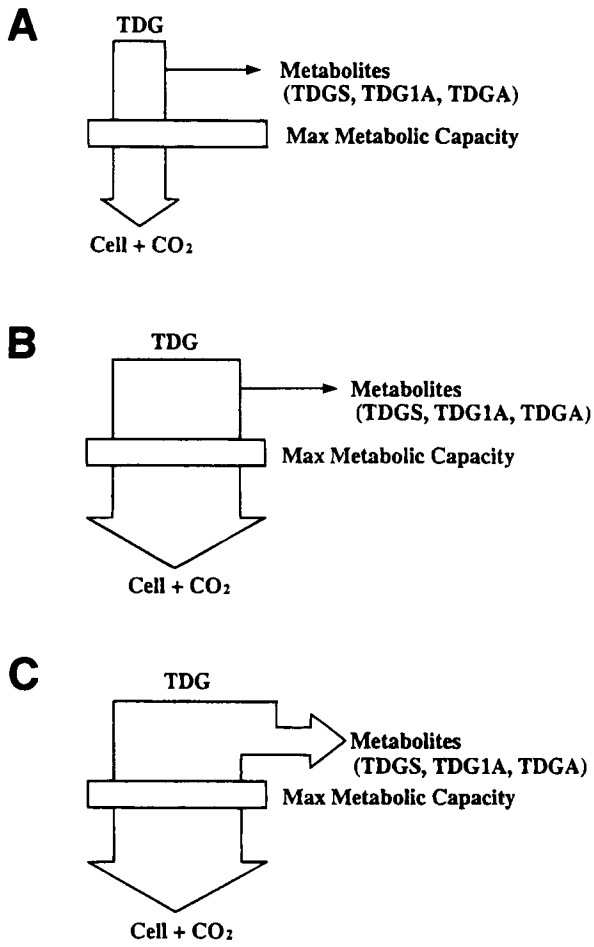

Fig. 8. Illustration of the bottleneck of the oxidative metabolism in SH91. **(A)** Excess oxidative capacity, and completely oxidative TDG to CO_2, TDG1A, TDGA, TDGS (for example, 30-m*M* batch: 2.4 m*M* [TDGS only] and 60-m*M* batch: 6.91 m*M* [TDGA+TDGS]). **(B)** The oxidative capacity is utilized completely. **(C)** Limit oxidative capacity, and the carbon flux is converted to byproducts by oxido-reductive metabolism (for example, 120-m*M* batch: 24.86 m*M* [TDG1A + TDGA + TDGS] and 170-m*M* batch: 84.36 m*M* [TDG1A + TDGA + TDGS]).

TDG. For the fed-batch case, with the proper feed rate, we should be able to minimize the TDG concentration, so that the cells consume TDG as it is added. Note, however, that the production of byproducts still occurs, and this method still exposes the cells to potentially high concentrations of byproducts, thus lowering the cell growth rate. The two-stage batch system improves upon this slightly in that the second-stage TDG addition effectively dilutes out the metabolite concentration, but does not expose the cells to too high a TDG level. Note also that this system was run with 500 m*M* initial TDG compared to 270 mM for the next-best fed-batch case. Thus, we found the 500-mM two-stage batch resulted in high degradation efficiency for

both paradigms. According to our experimental results, we suggest a two-stage or multistage fed-batch process may improve the degradation efficiency further, especially for high concentrations of TDG (500 m*M*, 61 g/L).

Finally, according to our experimental results and HPLC chromatogram analyses, we propose a metabolic capacity model for TDG degradation based on the known metabolic pathways (Fig. 1A). The model is shown in Fig. 8, and the metabolites produced by SH91 are dependent on the TDG concentration (or flux). Little metabolite is produced by SH91 at low initial TDG concentration (as shown in Fig. 8A). This is because the cells have enough capability to convert all TDG to cell mass and CO_2. In Fig. 8B, the cell degradation flux is increased at higher TDG concentrations owing to an increase in capacity. However, metabolites were produced when TDG flux increased further and was higher than the cell maximum metabolic capacity (Fig. 8C). This phenomenon then directly affected the cell mass yield. The yield factor became smaller when TDG flux increased over maximum degradation capacity. A more complex structured metabolic flux model is presently under consideration in our laboratory for describing SH91 growth on TDG.

ACKNOWLEDGMENT

The partial support of the US Army Edgewood, Research Development and Engineering Center is gratefully acknowledged.

REFERENCES

1. Somani, S. M. (1992), *Chemical Warfare Agents*, Academic, London.
2. Yang, Y.-C., Szafraniec, L. L., Beaudry, W. T., and Ward, J. R. (1988), *J. Org. Chem.* **53(14),** 3293–3297.
3. Sutherland, R. G. (1991), in *Verification of Dual-Use Chemicals Under the Chemical Weapons Convention: The Case of Thiodiglycol*, Lundin, S. J., ed., Oxford University Press, New York, p. 32.
4. Bentley, W. E., Bunnett, J. F., DeFrank, J. J., Fahnestock, M. V., Haley, M. V., Harvey, S. P., Isaacson, J. J., Kilbane, J. E., Kolakowski, M. P., Labare, J.-L., and Ontiveros, J. R. (1994), in Proceedings of the 1993 Scientific Conference on Chemical Defense Research, Aberdeen Proving Ground, Maryland pp. 1133–1138.
5. Lee, T.-S., Pham, M. Q., Weigand, W. A., Harvey, S. P., and Bentley, W. E. (1996), *Biotechnol. Prog.*, **12,** 533–539.
6. Pham, M. Q., Weigand, W. A., Harvey, S. P., and Bentley, W. E. (1995), *Appl. Biochem. Biotechnol.*, **57/58,** 779–789.
7. Black, R. M., Brewster, K., Clarke, R. J., Hambrook, J. L., Harrison, J. M., and Howells, D. J. (1993), *Xenobiotica* **23,** 473–481.
8. Zulty, J. J., DeFrank, J. J., and Harvey, S. P. (1994), in Proceedings of the Scientific Conference on Chemical and Biology Defense Research, Edgewood Research Development and Engineering Center, p. 68.
9. Lee, T.-S. (1994), Using *Alcaligenes xylosoxidans xylosoxidans*, (SH91) to degrade thiodiglycol, the product of sulfur mustard hydrolysis, M.S. thesis. University of Maryland, College Park, MD.
10. Andrews, J. F. (1968), *Biotechnol. Bioeng.* **10,** 707–723.